The Thesis Committee for Sotiris Komodromos
Certifies that this is the approved version of the following thesis:

Extraction of useful signals from noise using advanced time-frequency analysis in Enhanced Oil Recovery

APPROVED BY
SUPERVISING COMMITTEE:

Supervisors:

Nanshu Lu

Co-supervisor:

Dragan Djurdjanovic

Extraction of useful signals from noise using advanced time-frequency analysis in Enhanced Oil Recovery

by

Sotiris Komodromos

Thesis

Presented to the Faculty of the Graduate School of

The University of Texas at Austin

in Partial Fulfillment

of the Requirements

for the Degree of

MASTER OF SCIENCE IN ENGINEERING

The University of Texas at Austin

August 2017

Dedication

Στους γονείς μου που με δίδαξαν να προχωρώ μπροστά προσπερνώντας όλα τα εμπόδια στο δρόμο μου . Που σπούδασαν, έζησαν τον πόλεμο και τη προσφυγιά, έκαναν οικογένεια, μεγάλωσαν τα παιδιά τους, τα σπούδασαν και τους πρόσφεραν όσα ζήτησαν.

To my parents who taught me to keep moving forward regardless of the difficulties. Despite all the hardships my parents faced as refugees, they were determined to provide for their family and worked hard to rebuild what they had lost. Their efforts did not come easy, and they made many sacrifices, while always prioritizing family. I am reaping the benefits of their hard work and sacrifices and dedicate this thesis to them.

Acknowledgements

I would first like to thank my supervisor and lecturer Dr. Dragan Djurdjanovic. The door office was always open whenever I ran into a trouble or had a question about his classes, my research or writing. He steered me in the right the direction whenever he thought I needed it. Words are certainly not enough to express my gratitude to you.

I would also like to thank Dr. Nanshu Lu for happily accepting to be my co-supervisor, and I am gratefully indebted for her valuable comments on this thesis.

I must express my very profound gratitude to my parents, brother, sister and to my friends for providing me with unfailing support and continuous encouragement throughout my years of study. There were hardships and there will always be bumpy roads. It would have never been possible to keep moving forward without your support. Thank you.

Abstract

Extraction of useful signals from noise using advanced time-frequency analysis in Enhanced Oil Recovery

Sotiris Komodromos, M.S.E.

The University of Texas at Austin, 2017

Supervisors: Nanshu Lu

Dragan Djurdjanovic

In Enhanced Oil Recovery (EOR), the injected CO_2 does not distribute evenly through ground layers and often is not going to the desired direction. The key issue of this research, was to extract the useful signal from noise for a novel CO_2 subsurface imaging solution which uses surfaced based sensors only, in comparison with conventional seismic technology which requires downhole equipment [5, 7, 8, 19, 20]. That could potentially reduce the cost drastically due to its simplicity in installation, performance, less labor intensive and faster process of data. The extremely low signal-to-noise (S/N) ratio required the utilization of binomial time-frequency domains (TFDs) to process the collected field data as the problem involves extremely non-stationary signals. Binomial Cone-Kernel function is arguably the most advanced signal independent kernel; it allowed us to extract useful signals embedded in noise and observe repeatable waves for the first time.

Table of Contents

List of Tables

List of Figures

Chapter 1 Introduction

1.1 BACKGROUND

An oil reservoir is located at a depth below a series of porous and permeable rock layers, covered by an impermeable layer which is called caprock. An aquifer forms due to the water saturated porous and permeable layers. Over the years, water gets replaced by oil in certain locations and thus an oil reservoir is formed. The reservoir pressure is considered as hydrostatic due to the connection of the aquifer to the surface [1]. During drilling for oil, reservoir pressure of the oil column is less than the reservoir pore pressure and since oil is lighter than water, it allows the oil to flow to the surface naturally. When oil is removed from the reservoir during the production stage, the pressure and energy decrease and so does the production rate. The well production rate is a function of the pressure drawdown which is the difference of the pressure at the bottom and further from the well [1-4].

When the energy associated with the reservoir is not sufficient, in order to increase the recovery and maintain the desirable oil production, gas or water is injected to maintain the reservoir pressure and to sweep the oil towards the producers [1-5]. The implementation of such methods is called Enhanced Oil Recovery (EOR) and it involves many different techniques. This project considers the EOR process where CO_2 gas is injected. CO_2 is miscible with oil. The purpose of CO_2 injection is to change the capillary properties to mobilize the trapped oil in pores.[1-12]

Injected CO_2 does not distribute evenly through ground layers and often is not going to the desired direction. This leads to reduced production and waste of funds on unsuccessful CO_2 injections [1-12]. Mapping fluid migration allows the operator to evaluate different strategies to optimize the reservoir performance. Existing conventional seismic technologies can achieve this. However, these techniques are expensive and time

consuming. They require significant time for both data acquisition and processing, and in addition, production operations must be disrupted in order to run them. Computerized processes such as stacking, filtering and migrating are utilized to process raw seismic data into useable data [13-18]. Data processing can be very expensive and time-consuming. A typical analysis can take six months or even longer and the associated costs reach hundreds of thousands of dollars. [1-12]

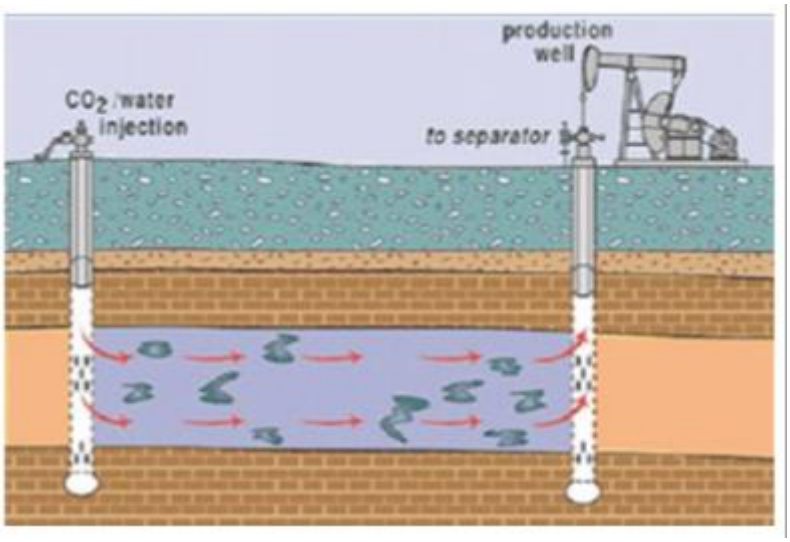

Figure 1: Carbon Dioxide EOR [4].

The key issue of the research presented in this MS thesis, is to extract the useful signal from noise for a different CO_2 mapping technology which uses surfaced based sensors only, compared to the conventional seismic technology which use downhole equipment [5, 7, 8, 19, 20]. That could potentially reduce the cost drastically due to its simplicity in installation, performance, less labor intensive and faster process of data. The extremely low signal-to-noise (S/N) ratio from energy scattering and absorption in the highly porous surface makes this problem very challenging [21]. The signals are weak compared to the large noise and thus very hard to recover [13-15]. The challenge is to

recover the signals embedded in noise and in this thesis, it is done utilizing advanced Cohen's class time-frequency analysis [22]. The next section discusses the organization of the thesis.

1.2 ORGANIZATION OF THE THESIS

The remainder of the thesis is organized as follows:

- Chapter 2 presents the literature review which covers the explanation of tube waves and guided waves that were investigated in this project. In addition, it covers the history and theory of Cohen's class time-frequency analysis which was the method applied.
- Chapter 3 covers the field and equipment setup used for data acquisition and how data processing was performed.
- Chapter 4 presents and discusses the results obtained using time-frequency analysis.
- Chapter 5 discusses conclusions and presents suggestions for future work.

Chapter 2 Literature Review

This review of the literature attempts to familiarize the reader with the signals of interest, which include tube waves generated in the source well, converted into laterally propagating guided waves and convert back to tube-waves in the receiver well. A brief explanation of these waves follows in Section 2.1 and Section 2.2 offers a brief review of Cohen's time-frequency analysis used for processing acoustic signals collected during this study.

2.1 TUBE WAVES AND GUIDED WAVES FOR OILFIELD APPLICATIONS

A tube wave is an interface wave which propagates down cased wellbores through two media, typically a borehole fluid and the wall of the surrounding elastic rock (interface between the fluid and the wall of the wellbore) [12]. They are usually considered as a source of noise due to their reflected late time arrival in the borehole seismic data [8, 11, 19, 23-28]. Thus, it is a standard procedure to eliminate them from the recorded data. Their high amplitudes allow the wave to propagate long distances with little energy loss [12, 19, 23-27]. Based on the definition provided at the Schlumberger Limited online oilfield glossary [12], "because the tube wave is coupled to the formation through which it is propagating, it can perturb the latter across open fractures intersecting the borehole". This squeezing effect potentially yields secondary tube waves that propagate both up and down from the fracture location [8, 11, 12, 19, 23-28]. Such events can be indicative of the presence of open fractures and their amplitude are related qualitatively to the length and width, i.e. the volume of the fluid-filled fracture space[12, 29]. Shallow formations where the overburden pressure is lower, generally suffer from this effect. [8, 11, 12, 19, 23-28]

A guided wave is a type of elastic wave that propagates and the surrounding low velocity beds are acting as waveguides. Many researchers have utilized guided waves to predict discontinuity and continuity of reservoir structures between wells[23, 30]

The Krauklis wave ("K-Wave") is a low frequency sound energy transmitted, late arrival seismic wave. Dr. Pavel V. Krauklis was the first to predict the existence of these waves in 1962 and they were later recorded by the Lawrence Berkeley National Laboratory (LBNL) amidst late arrival seismic data. According to Frehner [31], it has a dominant characteristic frequency compared to conventional seismic waves and can repeatedly propagate back and forth along a fracture and eventually fall into resonance emitting a seismic signal [31]. Historically, it has been considered as noise by the industry. [32, 33]

The cross well seismic data relevant to this research, have the trajectory as shown on Figure 2. Tube waves are generated in the source well and later converted into laterally propagating waves [20] due to hydraulic conductivity through the reservoir in gas/water layers, which convert back to tube-waves in the receiver well [19].

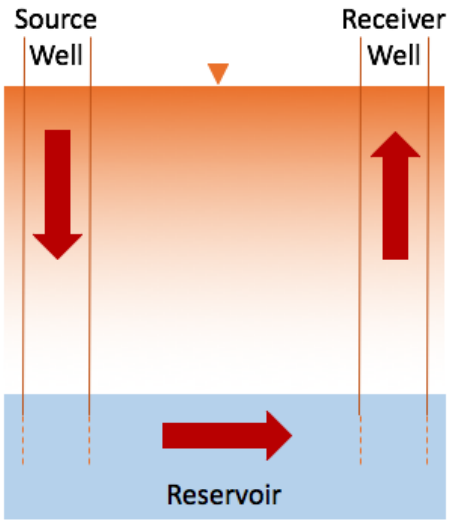

Figure 2: Cross well scheme and wave paths trajectory.

However, representing a system with a single input signal and a single output signal like on Figure 2 seems too simplistic for any real application [5]. It is expected that in any oilfield there will be multiple reflected waves with different paths[23, 28, 30, 34]. Possible scenarios are illustrated on Figure 3. On Figure 3 (a), the signal travels through reservoir, on (b) a direct wave propagates on the surface and (c) multiple waves reflect on different geologic strata. Most likely all three hypotheses take place.

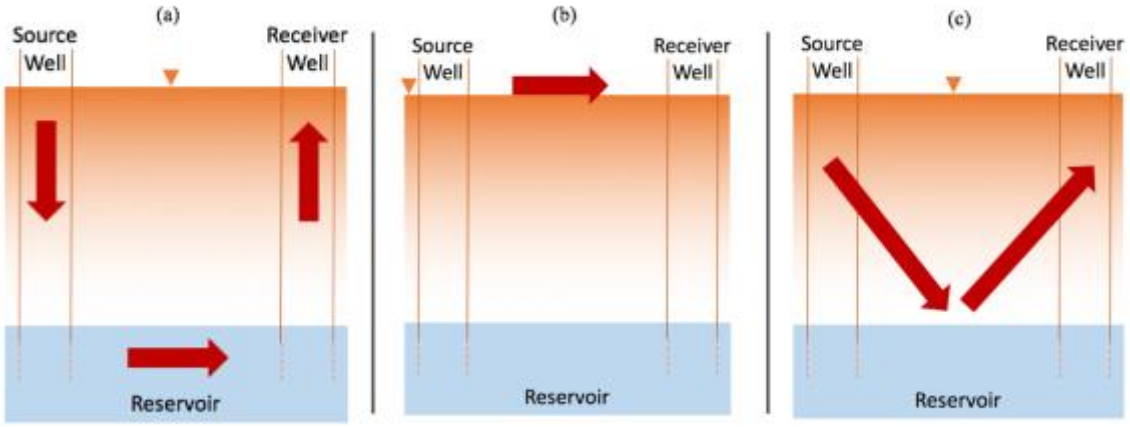

Figure 3: Possible hypothesis of the signal trajectory.

2.2 COHEN'S CLASS TIME-FREQUENCY STATIONARY SIGNAL ANALYSIS

Most signals in nature are highly non-stationary signals, with frequency content varying over time. An aircraft engine transitioning from one regime of operation into another emits non-stationary vibrations and sounds because excitation caused by variable rotational speeds causes variations in the frequency contents of the signals. Most real life signals, such as speech, music, machine tool vibration, acoustic emission etc. are non-stationary signals, which places strong emphasis on the need for development and utilization of non-stationary signal analysis techniques, such as wavelets, or joint time-frequency analysis.

Most traditional time-domain or frequency-domain based monitoring techniques for monitoring of dynamic systems (bearings, gears, machine tools, engines, DC/AC motors and drives etc.) utilize stationary signal characterization methods, such as time-series modeling or Fourier domain analysis (modal and spectral analysis) [35]. These methods assume that frequency content of the signal does not change over time, smearing the information when various frequency components appear or disappear in the signal. In simple terms, one is aware of what frequencies exist in the signal, but not when they existed [22].

Figure 4 depicts inadequacy of applying a stationary signal processing technique, such as spectral analysis, to non-stationary signals such as simple frequency-hopping signals shown in Figure 4. Spectral analysis is able to discern the three sinusoids present in the signals, but is unable to deduce when each one of those sinusoids occurred. Therefore, when the order of sinusoids is altered, the spectrum is unable to detect this change, as indicated in the Figure.

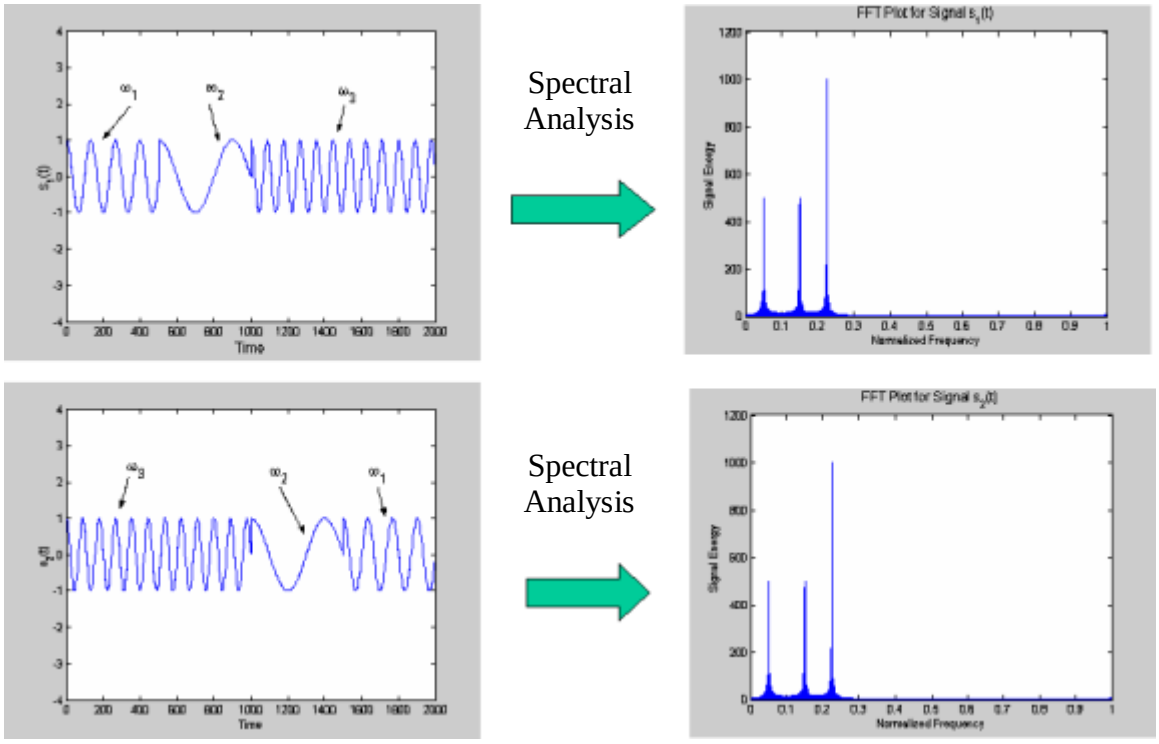

Figure 4: Application of Spectral analysis on two frequency hopping signals.

Applications based on the Wavelet signal transforms [36] have been used in geophysical seismic signal processing and interpretation for oil & gas exploration and production, petrophysical imaging for oil & gas reservoir, evaluation of hydrocarbon reservoirs, advanced seismic stratigraphy, high resolution subsurface imaging and modeling for complex earth media [36-42]. Even though wavelet techniques seem to be already a widely accepted method for processing and feature extraction in the presence of non-stationary, frequency varying signals [41, 43], advances in computing technology are slowly allowing a more intensive use of signal processing and feature extraction tools based on the Cohen's class of joint, time-frequency distributions [22, 44, 45].

The origins of this powerful signal description can be traced back to 1930s and advances in quantum physics in the work of Eugene Wigner [46] where he needed to

calculate a joint distribution of a particle having a given position and momentum. However, the position and momentum in quantum physics are connected through a Fourier transform, very much in the same way time and frequency contents of a signal are connected to the time-domain representation of the signal in the signal processing theory. This was noticed by a French engineer Ville [47], who realized that the same approach could be utilized to describe joint distributions of signal energy in both time and frequency.

At the same time spectrograms were developed independently. The time domain data is divided in shorter sub-sequences (windows) which usually overlap, and for each sequence, the calculation of the squared magnitude of the Fourier transform is made, giving frequency spectra for all windows. These frequency spectra are then ordered on a corresponding time-scale and form a three-dimensional picture (time, frequency, squared magnitude). The major problem with spectrograms is that it cannot be known how big the window should be. In addition, the windowing interferes with the signal. If a big window was used, a better spectral resolution could be achieved. But if a big window was used, the data got smeared in the time direction, which means if a bump was very short, it got smeared with a lot of things that did not happen with that bump. As a result, long windows yield a better frequency resolution with bad time resolution. If the window is shortened, a better time resolution is achieved but with very poor frequency resolution i.e. the frequency content will not be estimated well.

In 1966 Leon Cohen, a physicist, congealed these techniques into a comprehensive formulation known today as the Cohen's class time-frequency distribution. The formulation by Cohen was restricted with constraints of the ambiguity domain kernels in order to satisfy the so called Marginals. Cohen's class of time-frequency distributions for the signal $s(t)$ is defined as the triple integral,

$$C(t,\omega) = \frac{1}{4\pi^2} \int\int \varphi(\theta,\tau)\, A(\theta,\tau)\, e^{-j(\theta t+\tau\omega)} d\theta dt \qquad (1)$$

where

$$A(\theta,\tau) = \int s^*(t-\frac{\tau}{2})\, s(t+\frac{\tau}{2}) e^{j\theta t} dt$$

is the ambiguity function (signal independent kernel function of Doppler) of the signal and $\varphi(\theta,\tau)$ is the time-frequency kernel [22]. An intuitive interpretation of $C(t,\omega)$ is that it describes the energy distribution of $s(t)$ in time - t and frequency – ω [51]. In other words, the triple integral is the 2-D Fourier transform of the ambiguity domain.

The Reduced Interference Distribution (RID) time-frequency kernels, developed in mid 90-s at the University of Michigan [48, 49], represent a class of signal-independent, and therefore computationally less demanding, time-frequency kernels that result in time-frequency distributions (TFDs) whose favorable mathematical properties include [48, 49]: time-shift, frequency-shift and scale covariance properties, frequency and time marginal properties and instantaneous frequency and group delay properties. In addition, the RIDs have the property of suppressing the TFD cross-terms, which necessarily exist whenever multi-component signals are processed. Cross-terms are sometimes indistinguishable from the auto-terms and can hamper the time-frequency based signal interpretation and pattern recognition [44, 45]. Suppression of cross-terms is therefore a desirable mathematical property and RIDs achieve it in a signal-independent manner, which is computationally quicker to accomplish than the signal-dependent suppression pursued for example in [50].

On Figure 5, observe 2-D transformation because of the variables *t*, ω. Integrating $|s(t)|^2$ yields the Time Marginal and Integrating $|S(\omega)|^2$ yields the Frequency Marginal.

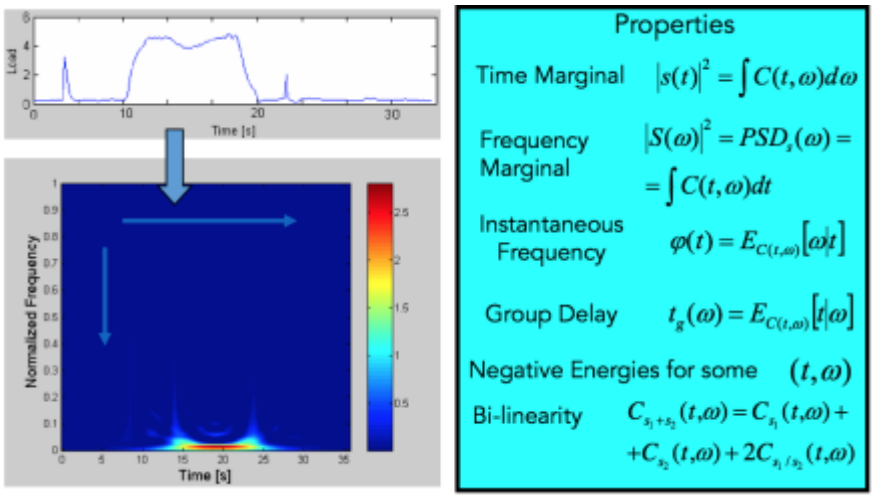

Figure 5: Two dimensional transformation and the mathematical properties of binomial distribution [51].

Figure 6 shows the RID signal energy distribution of the same signals shown in Figure 4. One can readily distinguish the 3 sinusoids present in the signal, as well as when those sinusoids existed. Figure 7 shows applicability of joint time-frequency signal analysis techniques to vibration signatures from a gearbox taken while gearbox was accelerating. Close observation of energy patterns in the time-frequency plane indicates a series of energy "bumps" that occur closer and closer together, and correspond to the mashing of the gear teeth. As it can be seen on the left chart, the signal was embedded in noise, however the processed data show clearly in a very high resolution the signal created by teeth machining in the gearbox. Another example, on Figure 8 observe the oscillations of tissue dampening created by a click of a jaw [51].

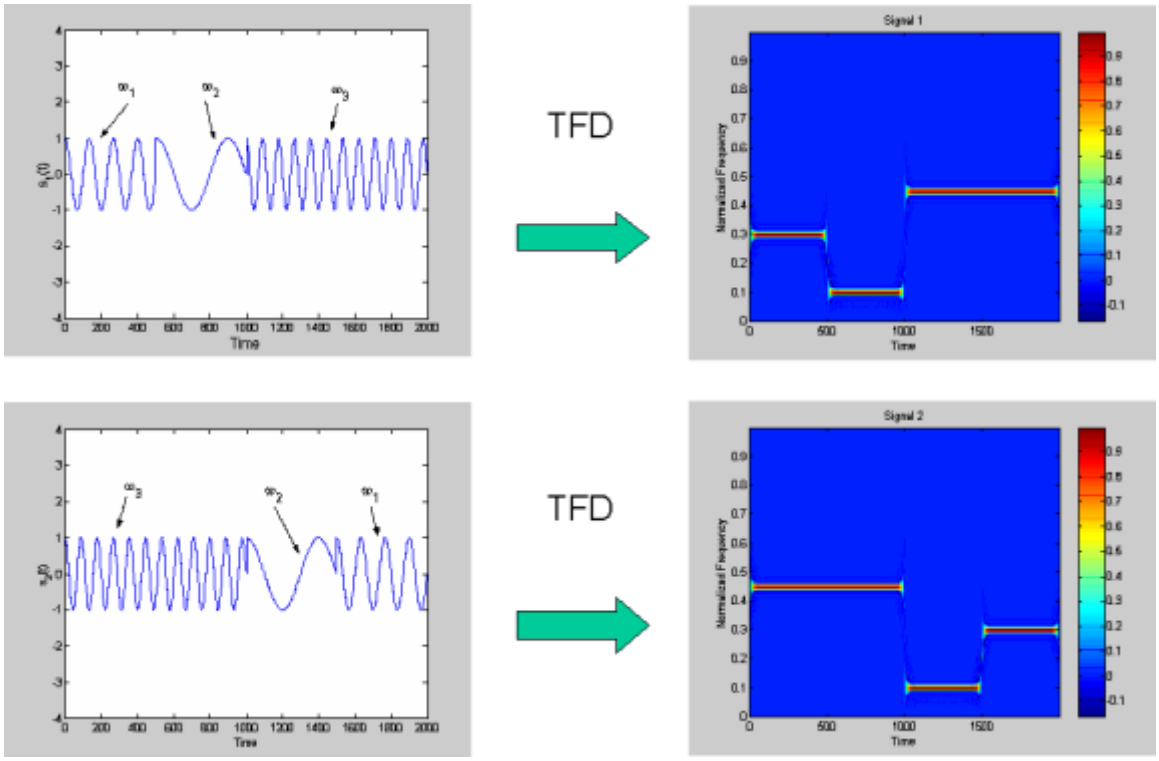

Figure 6: Reduced Interference joint time-frequency distribution of the two frequency hopping signals identical to those analyzed in Figure 4.

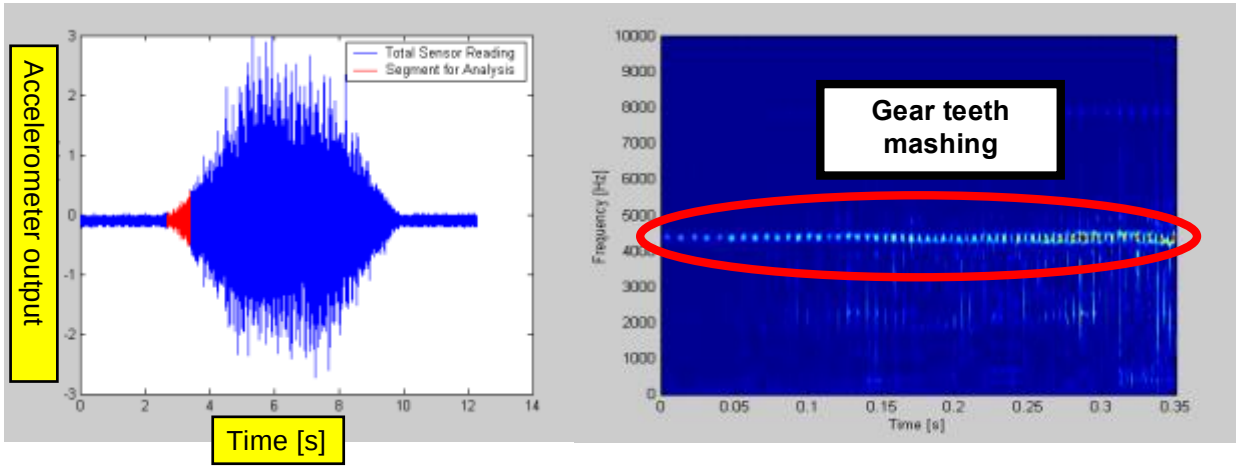

Figure 7: RID of gearbox vibrations emitted during acceleration of the gearbox.

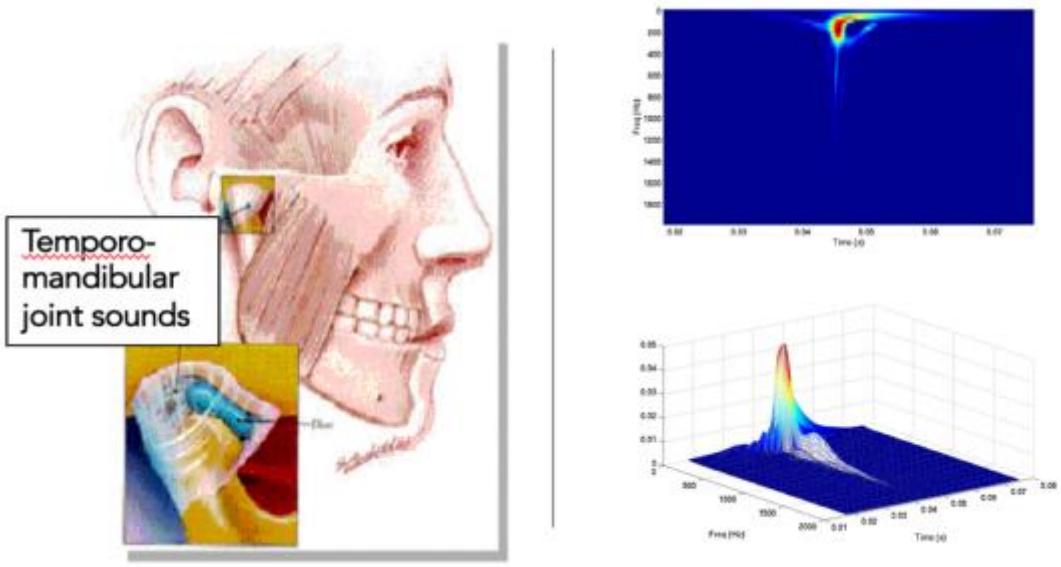

Figure 8: Example of Using Reduced Interference Cohen's Class Distributions [51].

Enhanced Oil Recovery (EOR) field data are extremely non-stationary. Seismic surveys which are often used in EOR, are conducted using external energy sources which induce vibrations. The seismic waves are generated usually by large vehicles also known as "Veibroseis trucks" which are equipped with heavy plates that vibrate on the ground or by special forms of blasting using explosives, such as dynamite [5, 52]. As discussed in the next chapter, the collected field data for this research involve a rapid release of CO_2, which results to an active pulse whose frequency content changes over time. Therefore utilization of Cohen's class of time-frequency distributions for the analysis of these data carries significant potential benefits. Stationary tools, such as Fourier analysis, or tools with limitations in terms of temporal and frequency resolutions, such as wavelets, may not be able to reveal minute details buried in often highly noisy signals.

2.3 NON-STATIONARY SIGNAL ANALYSIS METHODS FOR SEISMIC SIGNAL ANALYSIS

It is a common practice in seismic engineering to use the non-stationary analysis for the processing and interpretation of seismic signals [42]. Partyka et al. [54] applied short-time Fourier transform (STFT) to quantify thin-bed interference and detect subtle discontinuities within large 3-D surveys [55]. Chakraborty and Okaya showed that continuous wavelet transform (CWT) offers improved processing algorithms and spectral interpretation methods [56]. The S-transform proposed by Stockwell et al. [57], is a time-frequency analysis technique that combines elements of CWT and STFT, which has been widely applied on seismic data processing and the analysis of behavior of soil and structures. As discussed by Cheng et al. [58], a common issue of the classic symmetric Gaussian window is the degradation of time resolution in the time-frequency spectrum due to the long front taper. In addition they suggested an improved S transform with a bi-Gaussian window used to construct asymmetry bi-Gaussian windows.

Matching pursuit was also applied in seismic signal analysis to decompose seismic trace. Li and Zheng adopt Wigner–Ville distribution to carbonate reservoir characterization [59]. Liu et al. proposed a methodology to detect channels and low-frequency anomalies in seismic data using an inversion-based time-frequency [60]. Han and van der Baan [61] propose the instantaneous spectra combined with empirical mode decomposition for seismic data analysis. The synchrosqueezing transform (SST), provides a powerful method for analyzing signals with time-varying behavior. It was originally introduced for the analysis of audio signals and even today is powerful tool for time-frequency analysis. The main advantage of SST in comparison to traditional time-frequency methods, is its capability to analyze spectrally and decompose various types of signals with higher precision in time and frequency domain. Regardless of advances in computational resources, it is still computationally intensive method which requires further development.

The synchrosqueezed wavelet was applied transform to seismic time–frequency analysis and obtained significantly higher resolution than the WT. The synchrosqueezed wavelet transformcombines a classic wavelet analysis and a reallocation method of the time–frequency plane information to increase the spectral resolution [42, 57].

Chapter 3 Methodology

This chapter covers the different stages followed for the field data collection, including information regarding the field and equipment setup. The steps followed to process the data will be discussed at the end of this section.

3.1 DATA ACQUISITION SCHEDULE

Three wells were used for data acquisition, where one was an injector well and the other two were producing wells. All three CO_2 flooded. The source was mounted on the flowline of the injector well and the hydrophone receivers were mounted on the flowline of the two producing wells.

The source consists of a control unit operated using a laptop via WiFi. A main control valve on the source, opens and closes at about 100 psi. In this project, the source was releasing CO_2 upon opening. The hydrophone sensor was installed on the wellhead using a hookup. A preamp cable (3 channels) was connected to the sensor and the digitizer where the data are stored.

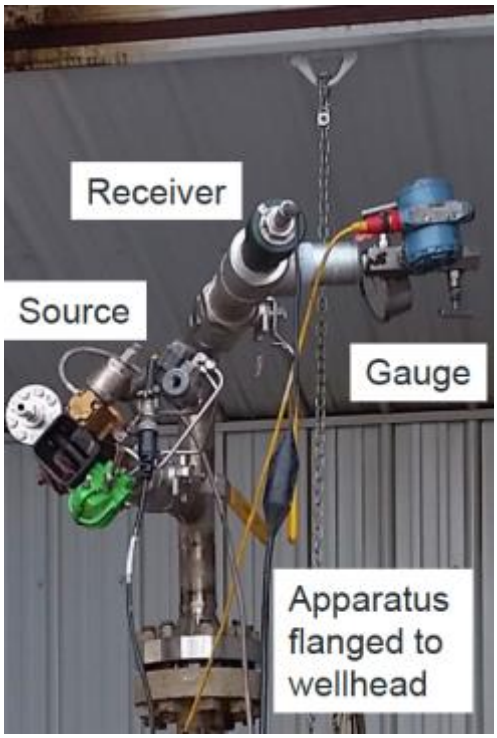

Figure 9: Equipment synopsis – Injector well with the source and receiver installed on the flowline.

Figure 10 demonstrates the layout of the cross wells, their relevant depths and distances from each other.

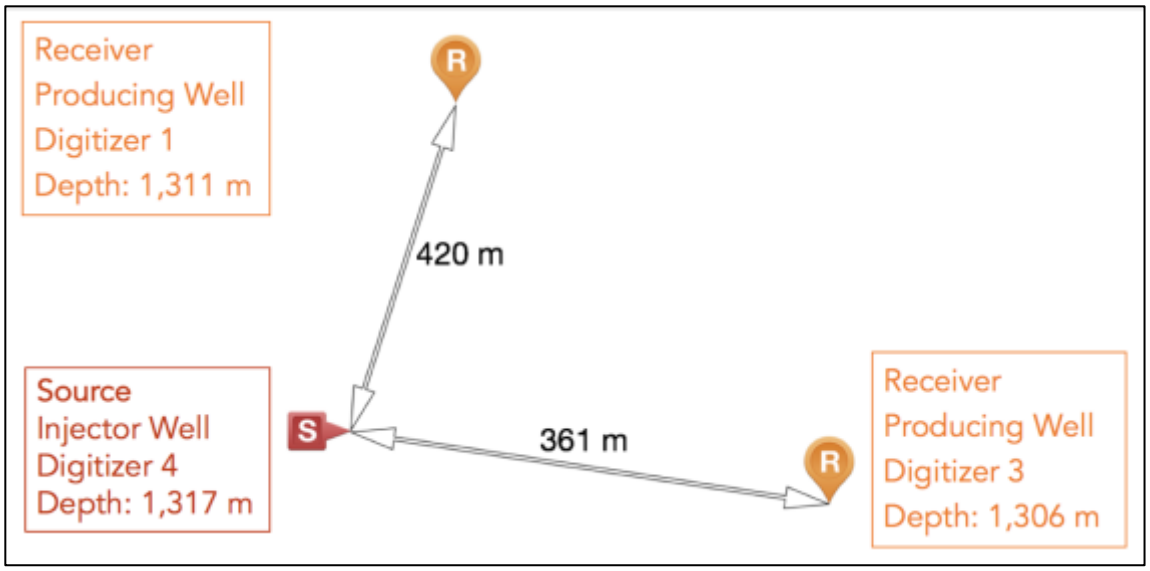

Figure 10: Layout distances.

Every time the valve opened on the source, CO_2 was released and created an active pulse. As a result, a change in pressure and energy occurred. In total, there were 72 active pulses with an interval time of approximately 45 seconds. The sampling rate was 4 kHz.

3.2 PROCESSING

Binomial TFDs were used to process the collected field data as the problem involves extremely non-stationary signals. Once the CO_2 gets released, an active pulse is created. The raw data were imported from the digitizer to the computer. Matlab was used to process the data.

The source data after its activation can be seen on Figure 11. Each active pulse was processed as a different time series i.e. the first 45 seconds was representing one time series and from 45 to 90 seconds a different time-series. In other words, each active pulse and its 45 duration was processed individually.

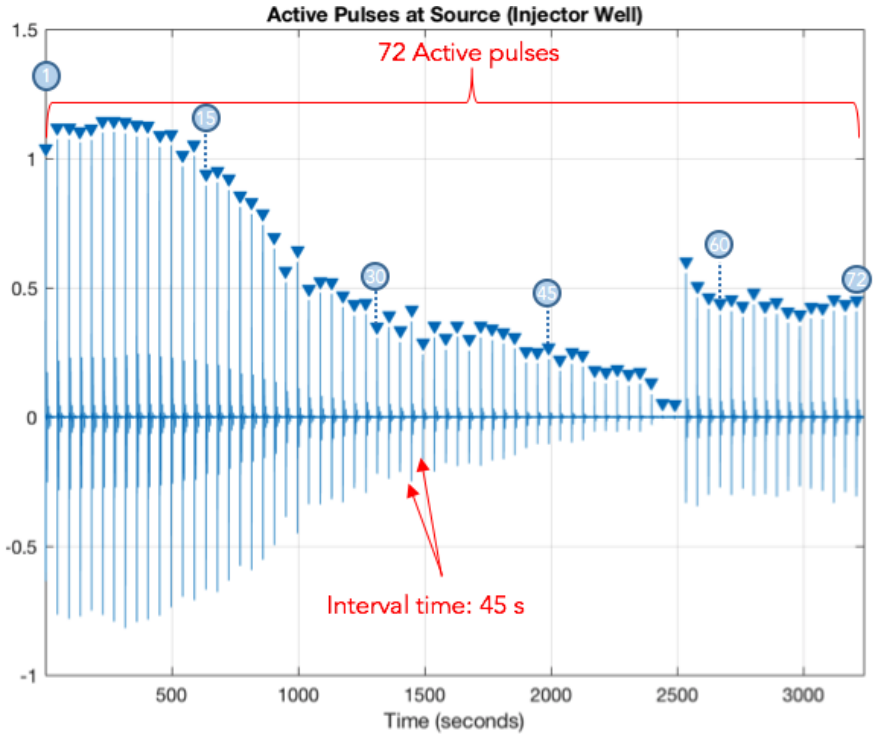

Figure 11: Raw data at source after source activation.

In Figure 12, the raw data of the first active pulse were plotted. Clearly, the signal is not visible through the noise. The data were analyzed at 160 Hz [62, 63] cause a higher rate would overwhelm the computing power available. The signals were processed using binomial kernel time-frequency domains. Binomial Cone-Kernel function is arguably the most advanced signal independent kernel [22, 49, 50, 53, 64, 65].

Lastly, visual inspection and manual procedures were used to observe the signals and their time of appearance was recorded. These observations will be presented and discussed in the next chapter.

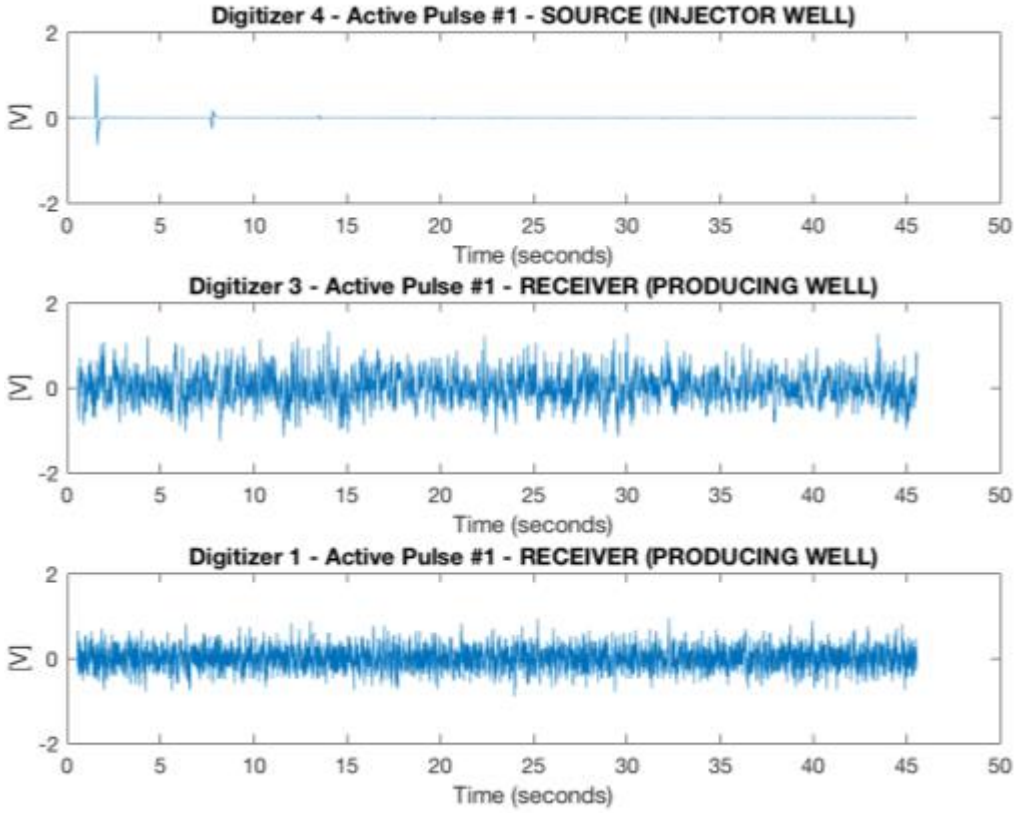

Figure 12: Raw data from Active Pulse #1.

Chapter 4 Results

In this chapter, the first fifteen active pulses will be processed and analyzed in detail. The charts consist of three subplots where the top represents the source and below the two receiver wells.

In Figure 13, the red arrows point at the detected signals (refer to Figure 10 for the layout of the field). To identify the "bumps", the figure was zoomed on Matlab and was visually inspected. The spider web structures is noise. The "bump" has a structure and it represents a bounce. For example, for the receiver connected to Digitizer 3 which is represented on the second plot of the figure, the first "bump" is detected at 4.26 seconds after the first active pulse at the source. Table 1 summarizes the time readings that were visually observed using Figure 13. Figure 14 and Table 2 are the corresponding results from the second trigger of the source. Note that on Figure 14 the time on the x axis continues since $t_0 = 0$ seconds, which is at the first trigger of the source.

ACTIVE PULSE #1	TIME ELAPSED (seconds)			
	1st Signal	2nd Signal	3rd Signal	4th Signal
Digitizer 3	4.26	6.57	10.71	26.44
Digitizer 1	4.43	7.85	9.08	14.83

Table 1: "bumps" detected by observing Figure 13

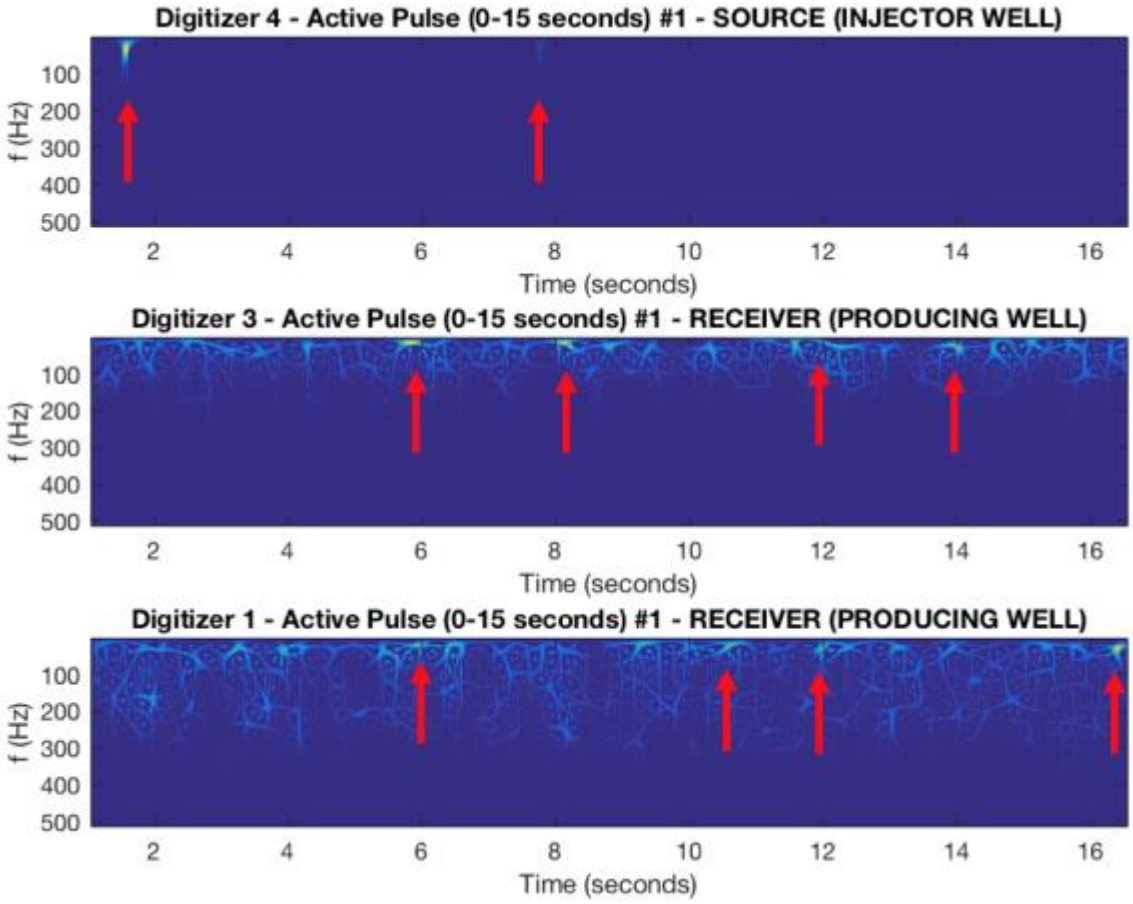

Figure 13: Active Pulse #1 - Processed data.

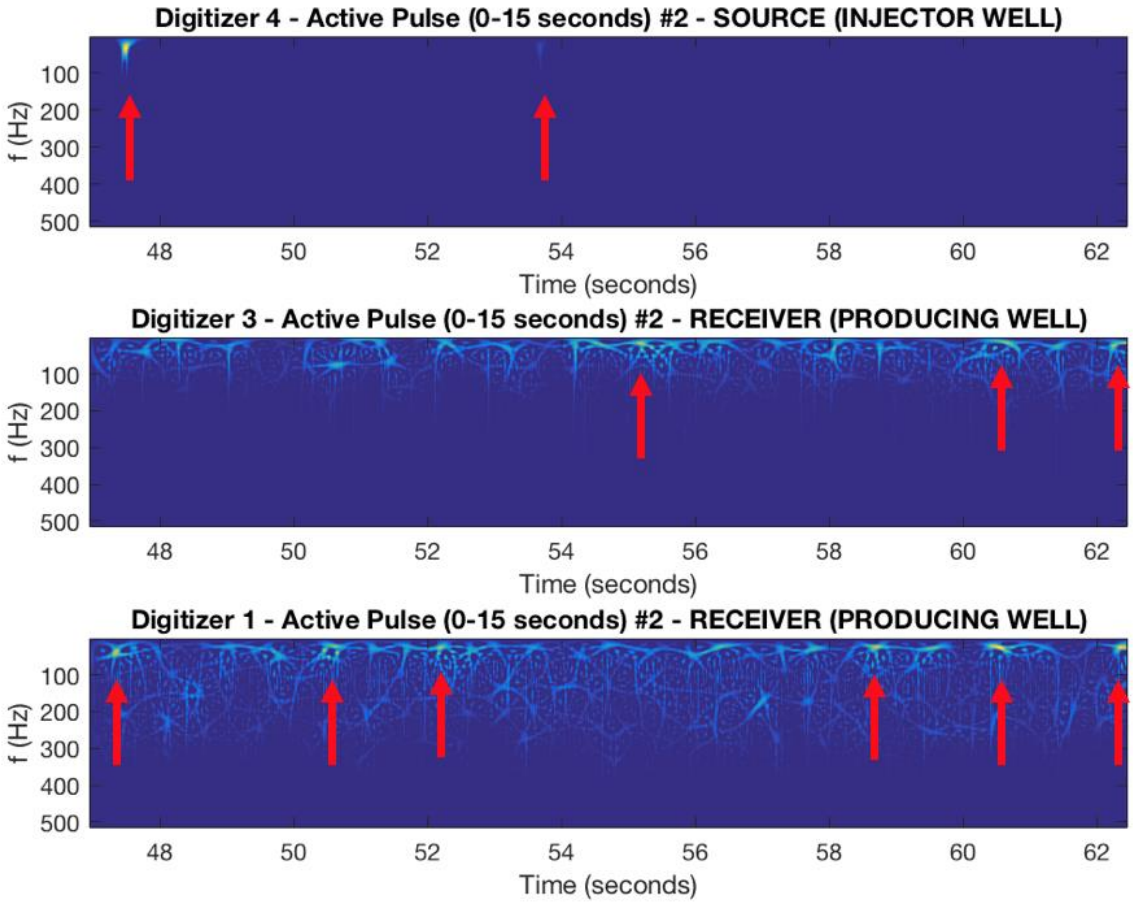

Figure 14: Active Pulse #2 - Processed data.

ACTIVE PULSE #2	TIME ELAPSED (seconds)			
	1st Signal	2nd Signal	3rd Signal	4th Signal
Digitizer 3	7.68	10.57	13.19	13.79
Digitizer 1	-0.21	3.12	11.19	13.01

Table 2: "bumps" detected by observing Figure 14

The observed "bumps" for the first fifteen active pulses are summarized in the next section.

4.1 Summary of observed "bumps" for the first fifteen active pulses

Digitizer 1	TIME ELAPSED				
	1st Signal	2nd Signal	3rd Signal	4th Signal	5th Signal
ACTIVE PULSE #1	4.43	7.85	9.08	14.83	23.66
ACTIVE PULSE #2	-0.21	3.12	11.19	13.01	14.86
ACTIVE PULSE #3	-0.16	1.20	7.76	9.96	12.56
ACTIVE PULSE #4	-0.40	2.20	11.10	14.20	16.30
ACTIVE PULSE #5	0.20	12.70	25.00	37.80	38.40
ACTIVE PULSE #6	2.00	5.60	7.70	9.30	11.30
ACTIVE PULSE #7	1.00	6.00	8.30	15.60	16.70
ACTIVE PULSE #8	-0.30	6.00	7.20	11.40	16.60
ACTIVE PULSE #9	-0.60	2.30	10.10	11.90	12.90
ACTIVE PULSE #10	0.00	4.50	7.70	10.40	20.60
ACTIVE PULSE 11	4.10	4.90	18.50	21.40	31.20
ACTIVE PULSE 12	1.70	8.70	9.70	13.40	30.10
ACTIVE PULSE 13	12.40	10.80	15.10	20.50	25.50
ACTIVE PULSE 14	11.10	18.60	21.00	29.40	-
ACTIVE PULSE 15	5.00	7.50	8.30	12.60	27.00

Table 3: Time elapsed since active pulse to observe signal on receiver connected to Digitizer #1.

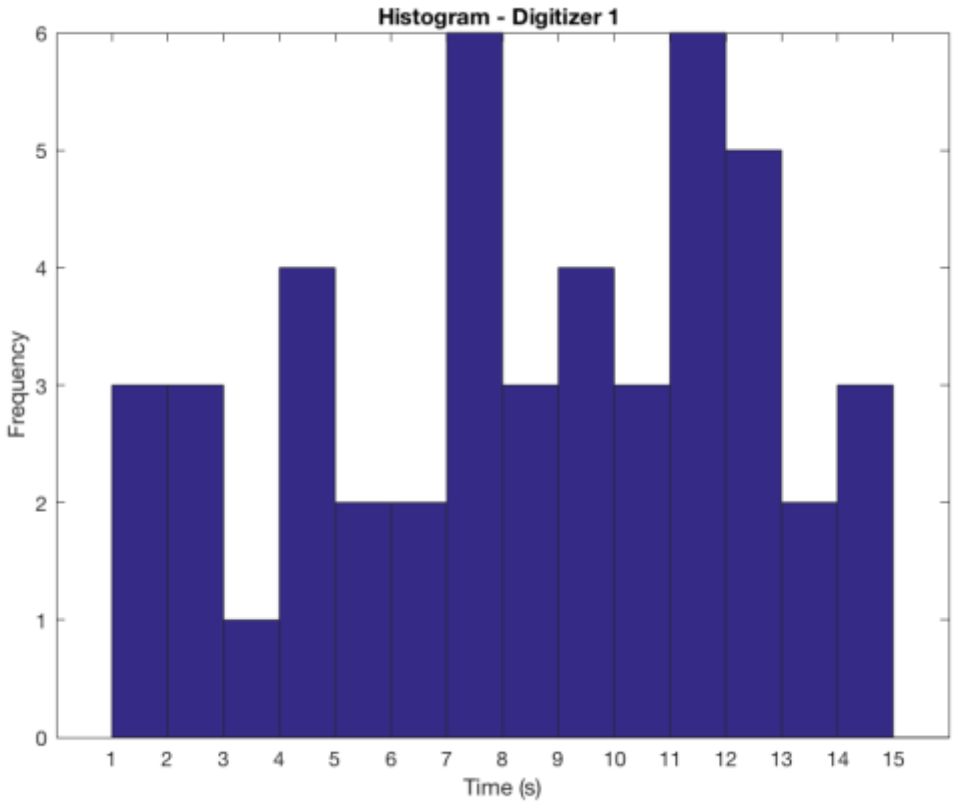

Figure 15: Histogram showing the number of times a "bump" was detected at Digitizer #1 well.

Digitizer 1	TIME ELAPSED				
	1st Signal	2nd Signal	3rd Signal	4th Signal	5th Signal
Average Value	2.68	6.80	11.85	16.38	21.26
Median	1.00	6.00	9.70	13.40	18.65
Standard Deviation	4.13	4.58	5.51	7.95	8.23

Table 4: Descriptive statistical results for Digitizer 1 well.

For the well where Digitizer 1 was positioned, the 1st bounce was observed in 15 out of 15 active pulses. Among the 15 active pulses, based on measurements the mean time was 2.68, the median was 1 and the sample standard deviation was 4.13. The 2nd bounce was observed in 15 out of 15 active pulses. Among the 15 active pulses, the mean time was 6.80, the median was 6.00 and the sample standard deviation was 4.58. The 3rd bounce was observed in 15 out of 15 active pulses. Among the 15 active pulses, the mean time was 11.85, the median was 9.70 and the sample standard deviation was 5.51. The 4th bounce was observed in 15 out of 15 active pulses. Among the 15 active pulses, the mean time was 16.38, the median was 13.40 and the sample standard deviation was 7.95. The 5th bounce was observed in 14 out of 15 active pulses. Among the 14 active pulses, the mean time was 21.26, the median was 18.65 and the sample standard deviation was 8.23. It is worth mentioning, that there were active pulses where more than five bounces were noticed. Moreover, observing the histogram at Figure 15, most of the bounces occurred between the 7^{th} and 8^{th} second, and 11^{th} to 12^{th} second since the trigger of the source. This is likely a good starting point for geological and geophysical analysis.

Digitizer 3	TIME ELAPSED				
	1st Signal	2nd Signal	3rd Signal	4th Signal	5th Signal
ACTIVE PULSE #1	4.26	6.57	10.71	26.44	34.91
ACTIVE PULSE #2	7.68	10.57	13.19	13.79	14.72
ACTIVE PULSE #3	9.16	12.46	17.46	-	-
ACTIVE PULSE #4	5.70	16.10	25.00	33.20	42.40
ACTIVE PULSE #5	10.20	10.80	14.50	31.90	32.80
ACTIVE PULSE #6	13.70	22.60	24.90	25.30	27.30
ACTIVE PULSE #7	5.90	6.60	8.20	6.50	15.90
ACTIVE PULSE #8	2.90	4.50	8.10	10.90	13.70
ACTIVE PULSE #9	1.10	3.70	7.40	10.90	17.00
ACTIVE PULSE #10	4.10	8.10	15.50	22.70	25.40
ACTIVE PULSE 11	11.10	15.40	24.90	-	-
ACTIVE PULSE 12	0.90	8.40	9.40	9.50	20.30
ACTIVE PULSE 13	15.40	16.70	18.20	-	-
ACTIVE PULSE 14	19.10	23.10	28.60	36.80	-
ACTIVE PULSE 15	16.10	27.30	28.30	-	-

Table 5: Time elapsed since active pulse to observe signal on receiver connected to Digitizer #3.

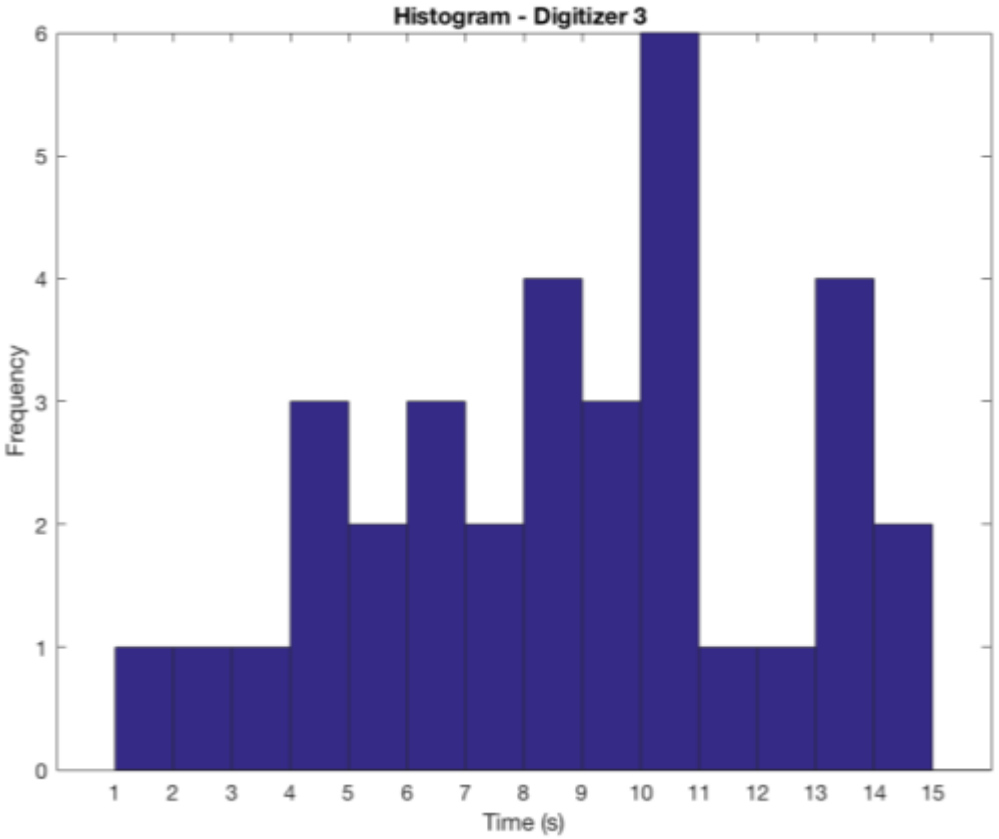

Figure 16: Histogram showing the number of times a "bump" was detected at Digitizer #3 well.

Digitizer 3	TIME ELAPSED				
	1st Signal	2nd Signal	3rd Signal	4th Signal	5th Signal
Average Value	8.49	12.86	16.96	20.72	24.44
Median	7.68	10.80	15.50	22.70	22.85
Standard Deviation	5.68	7.19	7.66	10.80	9.81

Table 6: Descriptive statistical results for Digitizer 1 well.

For the well where Digitizer 3 was positioned, the 1st bounce was observed in 15 out of 15 active pulses. Among the 15 active pulses, based on measurements the mean time was 8.49, the median was 7.68 and the sample standard deviation was 5.68. The 2nd bounce was observed in 15 out of 15 active pulses. Among the 15 active pulses, the mean time was 12.86, the median was 10.80 and the sample standard deviation was 7.19. The 3rd bounce was observed in 15 out of 15 active pulses. Among the 15 active pulses, the mean time was 16.96, the median was 15.50 and the sample standard deviation was 7.66. The 4th bounce was observed in 11 out of 15 active pulses. Among the 11 active pulses, the mean time was 20.72, the median was 22.70 and the sample standard deviation was 10.80. The 5th bounce was observed in 10 out of 15 active pulses. Among the 10 active pulses, the mean time was 24.44, the median was 22.85 and the sample standard deviation was 9.81. It is worth mentioning, that there were active pulses where more than five bounces were noticed. Moreover, observing the histogram at Figure 16, most of the bounces occurred between the 10^{th} and 11^{th} second since the trigger of the source.

These waves that appear on the results are coming from the multiple reflections as mentioned in the literature review (see Figure 3). There were time-series with more and less than five "bumps" appearing on the chart. Clearly, a tube-wave was generated at the source well. This can be justified with the repeatable reflection observed after 6.183 seconds in all 72 resulting charts. Taking in consideration the 1,317 m depth of the injector well where the source was, (see Figure 10) can estimate the velocity of the tube-wave. The reflection translates to the tube-wave travelling to the bottom of the well and up to the top, covering a distance of 1,317 m in 6.183 seconds. The tube-wave velocity is 426 m/s. [12] The result aggress with the predicted velocity (425-427 m/s) of the signal in CO_2 which is estimated based on the pressure and temperature of the well [24, 27]. Therefore, one can have confidence the observed "bumps" are caused by seismic waves. Where the oil and

CO_2 are based on the responses remains a question that geologists and geophysicists may try to answer, but this is beyond the scope of this thesis.

Chapter 5 Conclusions

5.1 CONCLUDING REMARKS

Utilization of binomial time-frequency domains enabled us to extract the useful signals embedded in noise where no other method could before this study. The repeatability and variability of those signals was analyzed. The results showed repeatable bounces. The multiple "bumps" appearing on the results could represent multiple reflections as mentioned in the literature review (see Figure 3). Identifying the paths is a very important task. However, it is beyond the scope of this thesis and requires geophysicist or a geologist to interpret the resulting processed data. As McFarland [5] said, "all seismic data is subject to interpretation, and no two experts will interpret data identically. Geology is still a subjective science" [5, 18]. The proper interpretation of the resulting data important information that could be useful in EOR [4, 5]. Various possibilities for future work based on this study will be discussed next.

5.2 RECOMMENDATIONS FOR FUTURE RESEARCH

A proposal for future work would be the creation of physical models. In addition, data mining techniques could be applied in order to automate the process of recording the time where a "bump" appears/ This would allow the process of all active pulses instead of only fifteen. This could potentially improve the interpretation of the processed data and exponentially reduce the required time compared to visual inspection.

Another proposal would be the process of the unstimulated data (before any tests were performed) which could provide valuable information regarding the ambient noise at the field.

Most importantly the interpretation of the resulting processed data should be done by a geologist or a geophysicist. The wave paths can be identified. A method that could be

applied to identify the paths, is influenced by the work represented in *Improvements in Capacitance-Resistive Modeling and Optimization of Large Scale Reservoirs* [3]. In oilfields, a tracer is added while pumping the wells. On this paper, a technology is described which is mainly for water flooding. The method relies on the rate changes and not the pressure changes like on this project. However, the equations could be modified to consider the parameters that serve the scope of this project. The rates of an injector well and the rates of a producing well always fluctuate. These rates are measured and can be correlated. This method could potentially be applied on this project to identify the wave paths. Using discrete element modeling (a simpler form of it) consisting of springs and dashpots in parallel can also potentially result to the wave paths.

References

[1] IFPEN - IFP School, TOTAL SA, IFP Training, Oil & Gas - From exploration to distribution, in: J.-M. Voirin (Ed.) Week 2 – V11 – Production Mechanisms and Hydrocarbon Recovery, IFP School, 2015, pp. 1-12.

[2] L.W. Lake, M. Walsh, A Generalized Approach To Primary Hydrocarbon Recovery Of Petroleum Exploration & Production, Elsevier Science BV, Amsterdam, 2003.

[3] D. Weber, T. Edgar, L. Lake, L. Lasdon, S. Kawas, M. Sayarpour, Improvements in Capacitance-Resistive Modeling and Optimization of Large Scale Reservoirs., Society of Petroleum Engineers (2009).

[4] RIGZONE, What Is EOR, and How Does It Work? . www.rigzone.com/training/insight.asp?insight_id=313. (Accessed July 25 2017).

[5] J. McFarland, How do seismic surveys work?, Oil and gas lawyer blog, Seismic Surveys, 2009

[6] M. Blunt, F.J. Fayers, F.M. Orr Jr, Carbon dioxide in enhanced oil recovery, Energy Conversion and Management 34(9–11) (1993) 1197-1204.

[7] J.B. Ajo-Franklin, J. Peterson, J. Doetsch, T.M. Daley, High-resolution characterization of a CO_2 plume using crosswell seismic tomography: Cranfield, MS, USA, International Journal of Greenhouse Gas Control 18 (2013) 497-509.

[8] T.M. Daley, L.R. Myer, G.M. Hoversten, J.E. Peterson, V.A. Korneev, Borehole Seismic Monitoring of Injected CO_2 at the Frio Site, 2006.

[9] T. Daley, R. Solbau, J. Ajo-Franklin, S. Benson, Continuous active-source seismic monitoring of CO_2 injection in a brine aquifer, GEOPHYSICS 72(5) (2007) A57-A61.

[10] T.M. Daley, J.B. Ajo-Franklin, C. Doughty, Constraining the reservoir model of an injected CO_2 plume with crosswell CASSM at the Frio-II brine pilot, International Journal of Greenhouse Gas Control 5(4) (2011) 1022-1030.

[11] E. Majer, T. Daley, V. Korneev, D. Cox, J. Peterson, J. Queen, Cost-effective imaging of CO_2 injection with borehole seismic methods, The Leading Edge 25(10) (2006) 1290-1302.

[12] Schlumberger Limited, The Schlumberger Oilfield Glossary, 2017. www.glossary.oilfield.slb.com. (Accessed June 24 2017).

[13] T. O'Haver, A Pragmatic introduction to signal processing, 1997, p. 146.

[14] A.V. Oppenheim, Discrete-time signal processing, Pearson Education India1999.

[15] A. Oppenheim, RES.6-008 Digital Signal Processing, 2011. https://ocw.mit.edu/. (Accessed September 15 2016 License: Creative Commons BY-NC-SA).

[16] C. Wood, L., S. Treitel, Seismic signal processing, Proceedings of the IEEE 63(4) (1975) 649-661.

[17] D. Mandic, M. Golz, A. Kuh, D. Obradovic, T. Tanaka, Signal processing techniques for knowledge extraction and information fusion, Springer2008.

[18] M. Landefeld, C. Hogan, Seismic Testing and Oil & Gas Production, The Ohio State University Extension.

[19] V. Korneev, J. Parra, A. Bakulin, Tube-wave Effects in Cross-Well Seismic Data at StrattonField, SEG Annual Meeting, Society of Exploration Geophysicists, Houston, TX, 2005, pp. 336-339.

[20] V.A. Korneev, Tube-wave seismic imaging, Google Patents, 2009.

[21] Ö. Yilmaz, Seismic Data Analysis, Investigations in Geophysics Seismic Data Analysis: Processing, Inversion, and Interpretation of Seismic Data, Society of Exploration Geophysicists2001.

[22] L. Cohen, Time-frequency Analysis, Prentice Hall PTR1995.

[23] A. Bakulin, V. Korneev, T. Watanabe, S. Ziatdinov, Time-lapse changes in tube and guided waves in cross-well Mallik experiment, SEG Technical Program Expanded Abstracts 2006, Society of Exploration Geophysicists2006, pp. 379-383.

[24] D.R. Bums, C.H. Cheng, Determination Of In-Situ Permeability From Tube Wave Velocity And Attenuation, Society of Petrophysicists and Well-Log Analysts, 1986.

[25] V. Korneev, A. Bakulin, S. Ziatdinov, Tube-wave monitoring of oil fields, SEG Technical Program Expanded Abstracts 2006, Society of Exploration Geophysicists2006, pp. 374-378.

[26] A.N. Norris, The speed of a tube wave, The Journal of the Acoustical Society of America 87(1) (1990) 414-417.

[27] S. Ziatdinov, A. Bakulin, B. Kashtan, V. Korneev, A. Sidorov, Tube-wave monitoring at Mallik field: comparing modeled and experimental time-lapse responses, SEG Technical Program Expanded Abstracts 2006, Society of Exploration Geophysicists2006, pp. 3240-3244.

[28] J.B.U. Haldorsen, D.L. Johnson, T. Plona, B. Sinha, H.-P. Valero, K. Winkler, Borehole acoustic waves, Oilfield review 18(1) (2006) 34-43.

[29] V. Korneev, Low-frequency fluid waves in fractures and pipes, Geophysics 75(6) (2010) N97-N107.

[30] J. Parra, C. Hackert, A. Gorody, V. Korneev, Detection of guided waves between gas wells for reservoir characterization, GEOPHYSICS 67(1) (2002) 38-49.

[31] M. Frehner, Krauklis wave initiation in fluid-filled fractures by seismic body waves, Geophysics 79(1) (2013) T27-T35.

[32] G. Goloshubin, V. Korneev, B. Kashtan, A. Bakulin, V. Troyan, G. Maximov, L. Molotkov, M. Frehner, S. Shapiro, R. Shigapov, Krauklis Wave-Half a Century After.

[33] V.A. Korneev, L. Danilovskaya, B.M. Kashtan, Krauklis Wave in Rock Fractures Filled with Fluid.

[34] R.i. Nolen-hoeksema, Beginner's guide to seismic waves, Oilfield Review 26(1) (2014).

[35] S.L. Marple, Digital spectral analysis: with applications, Prentice-Hall Englewood Cliffs, NJ1987.

[36] C.S. Burrus, R.A. Gopinath, H. Guo, Introduction to Wavelets and Wavelet Transforms: A Primer, Prentice Hall1998.

[37] S. Sunjay, Wavelets Transforms: Time–Frequency Presentation, GeoCanada 2010 – Working with the Earth, Calgary, Alberta, Canada, 2010.

[38] C. Liner, An overview of wavelet transform concepts and applications, University of Houston, 2010.

[39] M. Saadatinejad, H. Hassani, Application of wavelet transform for evaluation of hydrocarbon reservoirs: example from Iranian oil fields in the north of the Persian Gulf, Nonlinear processes in geophysics 20(2) (2013) 231-238.

[40] W. Liu, S. Cao, Y. Chen, Seismic Time–Frequency Analysis via Empirical Wavelet Transform, IEEE Geoscience and Remote Sensing Letters 13(1) (2016) 28-32.

[41] S. Sinha, P.S. Routh, P.D. Anno, J.P. Castagna, Spectral decomposition of seismic data with continuous-wavelet transform, GEOPHYSICS 70(6) (2005) P19-P25.

[42] P. Wang, J. Gao, Z. Wang, Time-Frequency Analysis of Seismic Data Using Synchrosqueezing Transform, IEEE Geoscience and Remote Sensing Letters 11(12) (2014) 2042-2044.

[43] R. Du, M.A. Elbestawi, S.M. Wu, Automated Monitoring of Manufacturing Processes, Part 2: Applications, 117(2) (1995) 133-141.

[44] W.J. Williams, Reduced interference distributions: biological applications and interpretations, Proceedings of the IEEE 84(9) (1996) 1264-1280.

[45] D. Djurdjanovic, J. Ni, J. Lee, Time-frequency based sensor fusion in the assessment and monitoring of machine performance degradation, Proceedings of the 2002 ASME International Mechanical Engineering Congress and Exposition, 2002.

[46] E. Wigner, On the Quantum Correction For Thermodynamic Equilibrium, Physical Review 40(5) (1932) 749-759.

[47] J. Ville, Théorie et Applications de la Notion de Signal Analytique, Cables et Transmissions Vol. 2A (1948) 61-74.

[48] J. Jeong, Time-Frequency Signal Analysis and Synthesis Algorithms, University of Michigan, 1990.

[49] J. Jeong, J.W. Williams, Kernel design for reduced interference distributions, IEEE Transactions on Signal Processing 40(2) (1992) 402-412.

[50] D.L. Jones, R.G. Baraniuk, An adaptive optimal-kernel time-frequency representation, IEEE Transactions on Signal Processing 43(10) (1995) 2361-2371.

[51] D. Djurdjanovic, S. Widmalm, W. Williams, C. Koh, K. Yang, Computerized classification of temporomandibular joint sounds, 47(8) (2010) 977 - 984.

[52] M. Sandsten, Time-Frequency Analysis of Time-Varying Signals and Non-Stationary Processes, Centre for Mathematical Sciences, Lund University, 2016.

[53] Q. Shie, C. Dapang, Joint time-frequency analysis, IEEE Signal Processing Magazine 16(2) (1999) 52-67.

[54] G. Partyka, J. Gridley, J. Lopez, Interpretational applications of spectral decomposition in reservoir characterization, The Leading Edge 18(3) (1999) 353-360.

[55] N. Zabihi, H.R. Siahkoohi, Single Frequency Seismic Attribute Based on Short Time Fourier Transform, Continuous Wavelet Transform, and S Transform.

[56] A. Chakraborty, D. Okaya, Frequency-time decomposition of seismic data using wavelet-based methods, Geophysics 60(6) (1995) 1906-1916.

[57] R.G. Stockwell, L. Mansinha, R.P. Lowe, Localization of the complex spectrum: the S transform, IEEE Transactions on Signal Processing 44(4) (1996) 998-1001.

[58] Z. Cheng, Y. Chen, Y. Liu, W. Liu, G. Zhang, H. Li, W. Chen, Seismic Time-frequency Analysis Using Bi-Gaussian S Transform.

[59] Y. Li, X. Zheng, Spectral decomposition using Wigner-Ville distribution with applications to carbonate reservoir characterization, The Leading Edge 27(8) (2008) 1050-1057.

[60] G. Liu, S. Fomel, X. Chen, Time-frequency analysis of seismic data using local attributes, Geophysics 76(6) (2011) P23-P34.

[61] J. Han, M. van der Baan, Empirical mode decomposition for seismic time-frequency analysis, GEOPHYSICS 78(2) (2013) O9-O19.

[62] L.T. Ikelle, L. Amundsen, Introduction to petroleum seismology, Society of Exploration Geophysicists2005.

[63] A.E. Barnes, The calculation of instantaneous frequency and instantaneous bandwidth, Geophysics 57(11) (1992) 1520-1524.

[64] P. Steeghs, G. Drijkoningen, Time-frequency analysis of seismic reflection signals, 1996 IEEE International Conference on Acoustics, Speech, and Signal Processing Conference Proceedings, 1996, pp. 2972-2975 vol. 5.

[65] F. Pérez-Cruz, O. Bousquet, Kernel methods and their potential use in signal processing, IEEE Signal Processing Magazine 21(3) (2004) 57-65.